



MOX-Report No. 04/2023

A mathematical model of the human heart suitable to address clinical problems

Quarteroni, A.; Dede', L.; Regazzoni, F.; Vergara, C.

MOX, Dipartimento di Matematica
Politecnico di Milano, Via Bonardi 9 - 20133 Milano (Italy)

mox-dmat@polimi.it

<https://mox.polimi.it>

A mathematical model of the human heart suitable to address clinical problems

Alfio Quarteroni, Luca Dede', Francesco Regazzoni, Christian Vergara

Received: date / Accepted: date

Abstract In this paper, we present a mathematical model capable of simulating the human cardiac function. We review the basic equations of the model, their coupling, the numerical approach for the computer solution of this mathematical model, and a few examples of application to specific problems of clinical interest.

Keywords Mathematical Modeling · Numerical Simulations · Applied Mathematics · Cardiac Modeling

Mathematics Subject Classification (2020) 65-M-XX, 65-N-XX

This work has been supported by the Italian research project MIUR PRIN17 2017AXL54F “Modeling the heart across the scales: from cardiac cells to the whole organ” and by the GNCS, “Gruppo Nazionale per il Calcolo Scientifico” (National Group for Scientific Computing) under the INdAM GNCS Project CUP_E55F22000270001.

Alfio Quarteroni

MOX - Dipartimento di Matematica, Politecnico di Milano, P.zza Leonardo da Vinci 32, 20133 Milano, Italy.

Mathematics Institute, École Polytechnique Fédérale de Lausanne (EPFL), Av. Piccard, CH-1015 Lausanne, Switzerland (*Professor Emeritus*)

E-mail: alfio.quarteroni@polimi.it

Luca Dede'

MOX - Dipartimento di Matematica, Politecnico di Milano, P.zza Leonardo da Vinci 32, 20133 Milano, Italy.

E-mail: luca.dede@polimi.it

Francesco Regazzoni

MOX - Dipartimento di Matematica, Politecnico di Milano, P.zza Leonardo da Vinci 32, 20133 Milano, Italy.

E-mail: francesco.regazzoni@polimi.it

Christian Vergara

LABS, Dipartimento di Chimica, Materiali e Ingegneria Chimica “Giulio Natta”, Politecnico di Milano, P.zza Leonardo da Vinci 32, 20133 Milano, Italy.

E-mail: christian.vergara@polimi.it

1 Introduction

The heart has always fascinated the best minds on our planet, through a long journey punctuated by brilliant insights and mistakes, which has seen some of the most extraordinary scientists and thinkers in our history try their hand: from Aristotle to Praxagoras, from Galen to Harvey, from Leonardo to Bernoulli and Euler.

The studies that we are conducting at the Politecnico di Milano (Italy) ideally fit into the groove traced by Euler. We are making an immaterial heart, made of equations capable of reproducing all vital cardiac processes – propagation of the electric signal, generation of microscopic forces at the cellular level, contraction and relaxation of the heart muscle, blood dynamics in atria and ventricles, myocardial perfusion due to coronaries, valve dynamics – as well as their interplay. Our research moves along studies conducted over the past decades, which have led to the development of increasingly detailed and predictive models [2, 3, 9, 10, 12, 13, 19, 27, 28, 29, 30, 31, 32, 34, 36, 39, 40, 45, 46, 47, 50, 51, 52, 56, 62, 63, 64, 66, 67, 68, 69, 71, 72, 73]. However, much remains to be done, both on the mathematical and numerical modeling.

If met, this challenge will provide an effective tool for qualitative and quantitative study of the cardiac function ([41, 42, 44]), under both physiological and pathological conditions, with the aim of contributing to its understanding, improving diagnostic analysis, and providing useful indications to targeted clinical treatments for specific cardiovascular diseases. The extraordinary complexity that determines the harmonious synchronization of the heart generating the heartbeat can be translated into equations (i.e., into a mathematical model) in virtue of the first principles of Physics: Newton's laws, those of thermodynamics, chemical kinetics, Navier-Stokes for blood dynamics, and Maxwell's for electric field propagation, to mention some.

The corresponding coupled system of nonlinear partial differential equations features a multiphysics and multiscale (in space and time) nature. For its solution we need to develop efficient and accurate numerical methods to handle the coupled problems underlying the cardiac functions and the single cores, followed by algorithms that are properly designed for large-scale and parallel computing. Once the numerical solution is achieved, we have available those variables representing physical quantities, such as, e.g., action potential, myocardial deformation in the two phases of contraction and relaxation, blood pressure and velocity, and stresses on the leaflets of the four heart valves. Altogether, thousands or millions of quantitative information representing the solutions of the system that enable us to reconstruct the complete state of the heart function at every millisecond of the heartbeat. A description such as, no medical images investigation would allow us to do so. But we can also do scenario analysis. What would happen if a valve were replaced? Or if a cardiac resynchronization therapy (CRT, [1]) was applied? Or, again, if one coronary artery bypass procedure were adopted rather than another? All without intervention, that is, non-invasively. A dream, of course, but we think we are not so far from its realization.

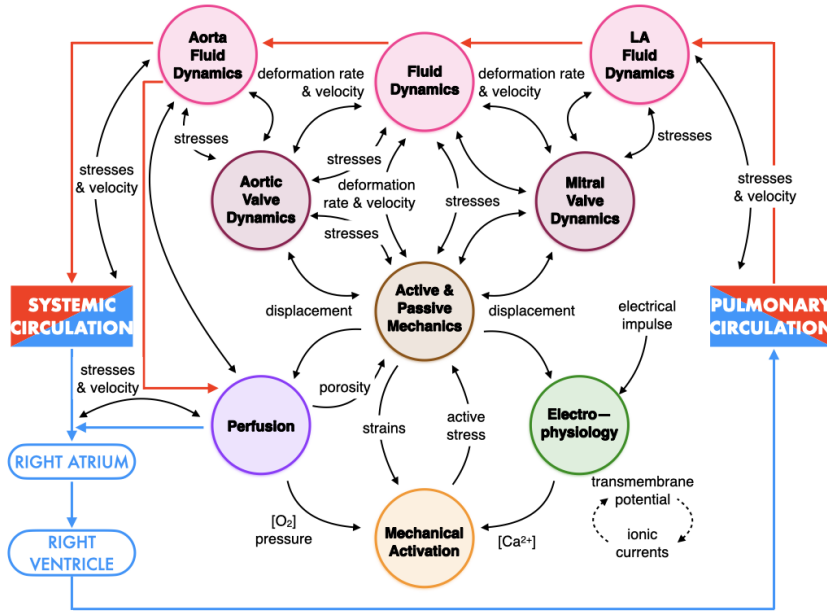


Fig. 1: Schemes of the physical processes underlying the cardiac function: detail of the left ventricle. Red and blue arrows indicate directions of oxygenated and deoxygenated blood flows; black arrows indicate exchange of physical quantities among physical processes.

In this paper, we will give a short account of our achievements in cardiac modelling and simulation. In Sect. 2 we will shortly describe the different physiological processes and the corresponding equations. In Sect. 3 we will present the main steps behind the numerical approximation. In Sect. 4 we will illustrate some examples of clinical applications. Finally, conclusions will be drawn in Sect. 5.

2 The physical processes and the corresponding equations

The physical processes and related basic equations underlying the cardiac function, sketched in Figure 1, are listed below (the mathematical models that translate these processes are called the *core models*). Electrophysiology, passive mechanics and perfusion problems as well as generation of microscopic forces will be written in a Lagrangian framework, thus in reference computational domain $\hat{\Omega}$, that is the space domain occupied by the myocardium in a load-free condition.

2.1 Cardiac Electrophysiology

Cardiac Electrophysiology is modeled by means of the so-called monodomain or bidomain equations, which are PDEs describing the propagation through the tissue of the action potential causing the excitation of cardiac cells [10, 61, 41]. These equations are coupled to suitable ionic models that provide a description of the ionic currents and sub-cellular mechanisms behind the excitation, expressed by a system of ODEs at every point in the computational domain. The interplay between tissue-scale and subcellular-scale processes is but one example of the multiscale nature of the phenomenon under consideration. Below we report the ODE system for the dynamics of ion concentrations (including calcium, sodium and potassium) and opening of ion channels, together with the bidomain model, which is a system of two evolutionary nonlinear diffusion-reaction equations for the simulation of the transmembrane and the extracellular potentials [10]:

$$\begin{cases} \frac{\partial \mathbf{w}}{\partial t} = \mathbf{F}_{\text{ion}}^{\mathbf{w}}(v, \mathbf{w}) & \text{in } \widehat{\Omega} \times (0, T] \\ \frac{\partial \mathbf{z}}{\partial t} = \mathbf{F}_{\text{ion}}^{\mathbf{z}}(v, \mathbf{w}, \mathbf{z}) & \text{in } \widehat{\Omega} \times (0, T] \end{cases}$$

$$\begin{cases} J\chi C_m \frac{\partial v}{\partial t} - \nabla \cdot (JF^{-1}D_i F^{-T} \nabla (v + v_e)) \\ \quad + J\chi I_{\text{ion}}(v, \mathbf{w}, \mathbf{z}) = J\chi I_{\text{app}}(\mathbf{x}, t) & \text{in } \widehat{\Omega} \times (0, T] \\ -\nabla \cdot (JF^{-1}D_i F^{-T} \nabla v) - \nabla \cdot (JF^{-1}(D_i + D_e) \nabla v_e) = 0 & \text{in } \widehat{\Omega} \times (0, T] \end{cases} \quad (1)$$

endowed with suitable boundary and initial conditions.

Notice the coupling of the two systems through the variables v , \mathbf{w} and \mathbf{z} , which reflects the multiscale and multiphysics nature of the process. Specifically, v describes the transmembrane potential, that is the potential difference between the inner and outer cellular space; \mathbf{w} is the set of gating variables, which describe the fraction of opened or closed ion channels; \mathbf{z} is the vector collecting the concentrations of the main ionic species. Finally, χ and C_m denote two properties of the cell membrane, namely the surface to volume ratio and the transmembrane capacitance.

We remark that the bidomain model of Eq. (1) is affected by the mechanical deformation of the tissue, through the terms $J = \det(F)$ and F – which we will introduce later in Sec. 2.3. These coupling stands at the basis of the so-called mechano-electric feedbacks [61, 68].

2.2 Generation of microscopic forces

One of the solution variables of the electrophysiology model is the intracellular calcium concentration, which is the main driver of the so-called excitation-

contraction coupling that leads to the generation of contractile force by muscular cells [41, 43, 58]. This process is captured by means of the RDQ20-MF force generation model [57], which is a very highly detailed model from the biophysical standpoint, and features an explicit description of sub-cellular mechanisms:

$$\begin{cases} \frac{\partial \mathbf{s}}{\partial t} = \mathbf{F}_{\text{act}} \left(\mathbf{s}, [\text{Ca}^{2+}]_i, SL, \frac{\partial SL}{\partial t} \right) & \text{in } \widehat{\Omega} \times (0, T] \\ SL = SL_0 \sqrt{I_{4f}} & \text{in } \widehat{\Omega} \times (0, T] \end{cases}$$

The vector \mathbf{s} collects variables describing the states of regulatory and contractile proteins responsible of the processes of force generation at the microscale. These processes are driven by the local calcium concentration (i.e. $[\text{Ca}^{2+}]_i$) and by the sarcomere elongation (i.e. SL), obtained as a function of the local tissue strain in the direction of cardiac fibers, as described below.

By solving this system of ODEs at every point in the computational domain $\widehat{\Omega}$, the force generation model computes an active stress tensor, which is added to the stress tensor for passive material properties of the cardiac tissue, in the so-called active stress framework:

$$P_{\text{act}}(\mathbf{d}, \mathbf{s}) = T_{\text{act}} \left(n_f \frac{F \mathbf{f}_0 \cdot \mathbf{f}_0}{\sqrt{I_{4f}}} + n_s \frac{F \mathbf{s}_0 \cdot \mathbf{s}_0}{\sqrt{I_{4s}}} + n_n \frac{F \mathbf{n}_0 \cdot \mathbf{n}_0}{\sqrt{I_{4n}}} \right),$$

$$T_{\text{act}} = T_{\text{act}}(\mathbf{s}, SL), \quad I_{4i} = F \mathbf{i}_0 \cdot F \mathbf{i}_0 \quad i \in \{\mathbf{f}, \mathbf{s}, \mathbf{n}\}.$$

Here and in the following, $\{\mathbf{f}_0, \mathbf{s}_0, \mathbf{n}_0\}$ denotes an orthonormal triplet of vectors spanning the whole computational domain and defining, respectively, the local orientation of cardiac fibers, fiber sheets and cross-fiber direction [5, 53]. The coefficients n_f , n_s and n_n tune the magnitude of active stress acting in the three orthonormal directions. Typically, $n_f > n_s$ and $n_f > n_n$ since most of the active tension is developed in the main direction of fibers.

2.3 Passive mechanics

The law of balance of momentum determines the mechanical strain of the myocardium, which models myocardial displacement due to interaction with blood, active forces generated by the electrical impulse, and passive response of the heart muscle [48, 33]. The latter two are described by the equations of elastodynamics for the sum of active and passive stress tensors, under the orthotropic constitutive assumption (i.e., with three preferred directions, i.e. fibers, collagen sheets, and direction perpendicular to the former):

$$\rho_s \frac{\partial^2 \mathbf{d}}{\partial t^2} - \nabla \cdot P_s(\mathbf{d}, \mathbf{s}) = \mathbf{0} \quad \text{in } \widehat{\Omega} \times (0, T], \quad (2)$$

where ρ_s denotes the tissue mass density. The passive stress tensor P_s is given by the sum of a passive and an active component [60, 17]:

$$P_s(\mathbf{d}, \mathbf{s}) = P_{\text{pas}}(\mathbf{d}) + P_{\text{act}}(\mathbf{d}, \mathbf{s}),$$

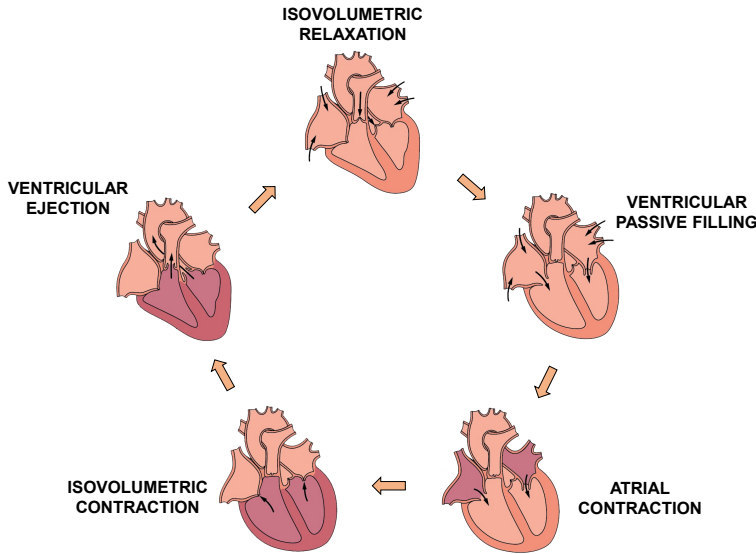


Fig. 2: Phases of the cardiac cycle.

where the passive stress tensor is obtained as the differential of a suitable strain energy density function \mathcal{W} [33,36]:

$$P_{\text{pas}}(\mathbf{d}) = \frac{\partial \mathcal{W}}{\partial F} \quad F = I + \nabla \mathbf{d}.$$

The strain energy density function \mathcal{W} defines indeed the passive behavior of the muscle tissue, and should be constitutively assigned in such a way it satisfied the principles of thermodynamics [33,36].

2.4 Blood flow dynamics

Each heartbeat results from the synchronized interaction between the contraction and relaxation of the four chambers and schematically involves two phases [41]: (i) the ventricular systole, with an initial isochoric phase and a subsequent phase of ventricular contraction in which the aortic and pulmonary valves open when the ventricular pressure exceeds the aortic and pulmonary pressures, respectively (in this phase there is ejection of blood to the systemic circulation); (ii) the relaxation phase (or ventricular diastole), during which a second isochoric phase caused by the closure of all four heart valves and characterized by a rapid fall in ventricular pressure is followed by the opening of the mitral and tricuspid valves and the expansion of the ventricles, resulting in a slow filling phase. This phase also includes atrial systole, which contributes to ventricular filling. See Figure 2.

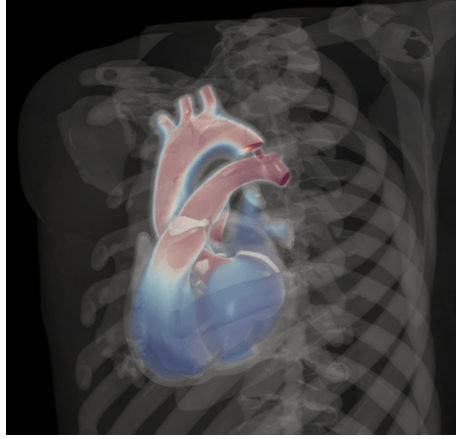


Fig. 3: Numerical simulation of blood flow dynamics in the whole heart (credits: A. Zingaro, Politecnico di Milano) [74].

These processes are described by the incompressible Navier-Stokes equations in a moving domain Ω_f , the one corresponding to the union of the four cardiac cavities (see Figure 4), having the blood velocity (\mathbf{u}) and pressure (p) as unknowns, yielding the so-called Arbitrary-Lagrangian-Eulerian (ALE) formulation [38, 4, 74]:

$$\begin{cases} \rho_f \left[\frac{\partial \mathbf{u}}{\partial t} + ((\mathbf{u} - \mathbf{u}_{\text{ALE}}) \cdot \nabla) \mathbf{u} \right] - \nabla \cdot \sigma_f(\mathbf{u}, p) = \mathbf{0} & \text{in } \Omega_f \times (0, T] \\ \nabla \cdot \mathbf{u} = 0 & \text{in } \Omega_f \times (0, T], \end{cases} \quad (3)$$

where the stress tensor σ_f is modeled by the Newtonian law:

$$\sigma_f(\mathbf{u}, p) = \mu (\nabla \mathbf{u} + \nabla \mathbf{u}^T) - pI,$$

with μ being the blood viscosity and where the ALE virtual fluid domain displacement is obtained as the solution of the following extension problem:

$$\begin{cases} -\nabla \cdot P_{\text{ALE}}(\mathbf{d}_{\text{ALE}}) = \mathbf{0} & \text{in } \widehat{\Omega}_f \times (0, T] \\ \mathbf{d}_{\text{ALE}} = \mathbf{d} & \text{on } \widehat{\Sigma} \times (0, T] \end{cases} \quad \mathbf{u}_{\text{ALE}} = \frac{\partial \mathbf{d}_{\text{ALE}}}{\partial t},$$

where $\widehat{\Omega}_f$ is the reference domain and Σ the fluid-structure (blood-myocardium) interface (which physically corresponds to the endocardium). Notice the geometric coupling between fluid and structure through \mathbf{d} . Problems (3) and (2) are furtherly coupled by two continuity conditions on Σ stating no-slip condition and third Newton law [55].

Turbulence models are used to simulate laminar to turbulent transitional flow regimes, which may occur especially during left ventricular filling [6, 20, 75].

Figure 3 displays a numerical result of blood flow dynamics in the whole heart.

2.5 Valve dynamics

We model the rapid opening and closing of valve leaflets. A correct description of valve dynamics is necessary to break down the various phases of the heartbeat and properly describe the function of pumping blood through the circulatory system [24, 41]. In addition, much of the most common heart disease is associated with valvular dysfunction such as calcified stenosis and valvular regurgitation (so-called "heart murmur"). In our approach, we use the Resistive Immersed Implicit Surface (RIIS) method for the inclusion of cardiac valves [16]. This approach consists in adding an extra term to the momentum equations that penalizes the difference between the effective fluid velocity $\mathbf{u} - \mathbf{u}_{\text{ALE}}$ and the one of the valve leaflets \mathbf{u}_Γ ¹:

$$\rho_f \left[\frac{\partial \mathbf{u}}{\partial t} + ((\mathbf{u} - \mathbf{u}_{\text{ALE}}) \cdot \nabla) \mathbf{u} \right] - \nabla \cdot \sigma_f(\mathbf{u}, p) + \mathcal{R}(\mathbf{u}, \mathbf{u}_{\text{ALE}}) = \mathbf{0} \quad \text{in } \Omega_f,$$

where

$$\mathcal{R}(\mathbf{u}, \mathbf{u}_{\text{ALE}}) = \frac{R}{\varepsilon} \delta_\varepsilon(\varphi^t(\mathbf{x})) (\mathbf{u} - \mathbf{u}_{\text{ALE}} - \mathbf{u}_\Gamma),$$

R and ε are suitable constants, δ_ε is a smoothed Dirac delta function which depends on φ^t , which represents the distance function describing an immersed surface. This introduces an extra variable to describe the valve's kinematics. The latter could be provided by solving a reduced model driven by a blood-pressure jump across the valves themselves. This approach can be regarded as a simplified one if compared with a full 3D fluid-structure interaction (FSI) between blood and finite elasticity for valves, yet it allows capturing the macroscopic effect of valves on the flow, such as their role in determining the heartbeat phases, the way they prevent reverse flow, and the formation of jets and vortices due to the presence of valve leaflets [8].

2.6 Circulatory system

The circulatory system can be described by means of a lumped parameter model, representing through a system of ODEs the evolution of pressure and flow rate in several vascular compartments. The model is constructed thanks to an analogy to electrical circuits, whereby blood flow is likened to electric current, and pressure difference to potential difference. Through this analogy, vessel compliance is described by capacitors, blood friction is modeled by resistors, and inertia by inductance-type elements [7, 35, 59].

2.7 Myocardial perfusion

We model the process of cardiac perfusion, representing the blood and oxygen supply due to blood flowing in the coronary tree, from epicardial coronary

¹ Notice that here \mathbf{u}_Γ is not intended as the absolute valve velocity, rather as the relative valve velocity with respect to the myocardial motion

arteries (comparable to the organ scale) to capillaries (comparable to the cellular scale). The interplay between perfusion and contraction underlies some typical features of cardiac physiology, such as the phenomenon of coronary flow impediment that occurs during systole. However, here we neglect cardiac contraction for the perfusion modeling, as we only focus on the diastolic phase, where most of the perfusion occurs. In particular, perfusion modeling is obtained again by a coupled problem, namely 3D fluid-dynamics through Navier-Stokes equations for the large coronaries and multicompartment Darcy model for the intramyocardial coronaries and micro-circulation, under the modeling assumption that blood dynamics in the myocardium could be seen as the flow in a porous medium [14, 15, 37]:

$$\left\{ \begin{array}{ll} \rho_f \left[\frac{\partial \mathbf{u}}{\partial t} + (\mathbf{u} \cdot \nabla) \mathbf{u} \right] - \nabla \cdot \sigma_f(\mathbf{u}, p) = \mathbf{0} & \text{in } \Omega_{\text{cor}} \times (0, T] \\ \nabla \cdot \mathbf{u} = 0 & \text{in } \Omega_{\text{cor}} \times (0, T] \\ \mathbf{K}_i^{-1} \mathbf{u}_{\text{myo},i} + \nabla p_{\text{myo},i} = \mathbf{0}, \quad i = 1, 2, 3 & \text{in } \Omega \times (0, T] \\ \nabla \cdot \mathbf{u}_{\text{myo},1} = \sum_{j=1}^J \frac{\chi_{\Omega^j}}{|\Omega^j|} \int_{\Gamma_{\text{cor}}^j} \mathbf{u} \cdot \mathbf{n} - \beta_{1,2}(p_{\text{myo},1} - p_{\text{myo},2}) & \text{in } \Omega \times (0, T] \\ \nabla \cdot \mathbf{u}_{\text{myo},2} = -\beta_{2,1}(p_{\text{myo},2} - p_{\text{myo},1}) - \beta_{2,3}(p_{\text{myo},2} - p_{\text{myo},3}) & \text{in } \Omega \times (0, T] \\ \nabla \cdot \mathbf{u}_{\text{myo},3} = -\gamma(p_{\text{myo},3} - p_{\text{veins}}) - \beta_{3,2}(p_{\text{myo},3} - p_{\text{myo},2}) & \text{in } \Omega \times (0, T] \\ \sigma_f(\mathbf{u}, p) \mathbf{n} \cdot \mathbf{n} - \frac{1}{\alpha^j} \int_{\Gamma_{\text{cor}}^j} \mathbf{u} \cdot \mathbf{n} = \frac{1}{|\Omega^j|} \int_{\Omega^j} p_{\text{myo},1} & \text{on } \Gamma_j^{\text{cor}} \times (0, T] \end{array} \right.$$

Here, Ω_{cor} represents the large coronaries domain (supposed here to be rigid), Ω^j is j -th perfusion region in which the myocardium has been subdivided (see [11] and Figure 4, right), Γ_{cor}^j the outlet of j -th coronary which is at the interface with Ω^j (see [14]), J is the total number of perfusion regions, and p_{veins} the given venous pressure. The variables of the model are the blood velocity in the large coronaries \mathbf{u} and in the three Darcy compartments $\mathbf{u}_{\text{myo},1}$, $\mathbf{u}_{\text{myo},2}$ and $\mathbf{u}_{\text{myo},3}$; the pressure in the large coronaries p and in the three Darcy compartments $p_{\text{myo},1}$, $p_{\text{myo},2}$ and $p_{\text{myo},3}$. The parameters $\beta_{i,j}$, γ , \mathbf{K}_i and α^j are associated with the blood permeability between compartments. The last equation represents the third Newton law at the interface between the large coronaries and the first Darcy compartment Using the perfusion model, we can quantify the effect of coronary stenosis on perfusion, leading to a possible ischemic process and the effect of the latter on cardiac output (that is the blood ejection from the left ventricle into the ascending aorta through the aortic valve).

3 From modeling to solution

This mathematical model, being derived from physical laws, can be thought of as *universal*: it applies not only to a single heart but to every possible human heart. What differentiates one heart from another is data: geometric data (i.e., morphology, as each heart is different from the others), the material characteristics (fiber orientation, coefficients characterizing its elasticity and

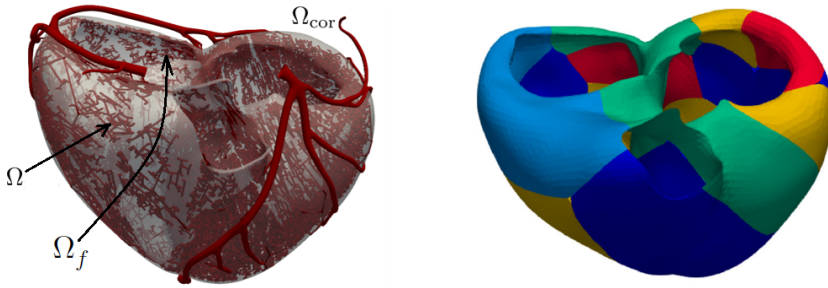


Fig. 4: Computational domains (left) and perfusion regions (right).

electrical conductivity), what happens at the “boundary” of the domain of interest (different pressure gradients or flow rate among patients), and the health status (e.g., the possible presence of specific pathologies, such as any scars, valvular insufficiencies, cardiomyopathies, ...). These data, which vary from patient to patient, are the input to the universal model, and the latter will output results in terms of blood velocity and pressure, myocardial and valve displacements, and transmembrane potential (the unknowns of the above core cardiac models) that will themselves be patient-specific.

The source of morphological data are medical images used in common clinical practice, such as magnetic resonance imaging (MRI) or computed axial tomography (CT). In the cardiac field, MRI is used to acquire cine-MRI type series - that is, dynamic images that allow reconstruction of the shape and motion of the heart chambers (which we will use for hemodynamic simulations) - and Late Gadolinium Enhancement (LGE)-type series - that through the use of contrast medium allow reconstruction of scars and fibrotic areas of cardiac tissue (which we will use for simulation of heart rhythm pathologies). CT, on the other hand, due to its better spatial definition, can be used to reconstruct not only cardiac chambers, but also small vessels such as coronary arteries and valve leaflets. Figure 5, left, illustrates the result of the reconstruction (using mathematical algorithms [53]) of the cardiac fibers of the myocardium. The fibers conduct the electrical signal and enable optimal contraction and torsion of the heart muscle in the systolic phase. Regarding dynamic data used for boundary conditions, they could come, e.g., from EchoColor Doppler acquisitions, whereas electrical data needed to calibrate the conduction velocity of electrical propagation or to prescribe boundary conditions could be obtained by invasive mapping procedures.

Once our problem is set upon rigorous mathematical ground, and the relevant data (boundary conditions, initial conditions, problem’s coefficients) are provided, the next step consists of reducing it to a finite dimension, say N (typically very large, of an order of millions or more). A mathematically rigorous strategy consists in projecting, at any time, the variational (weak) formulation of the differential system onto finite-dimensional subspaces of the Sobolev spaces the weak solution of the original system belongs to. For the sake of il-

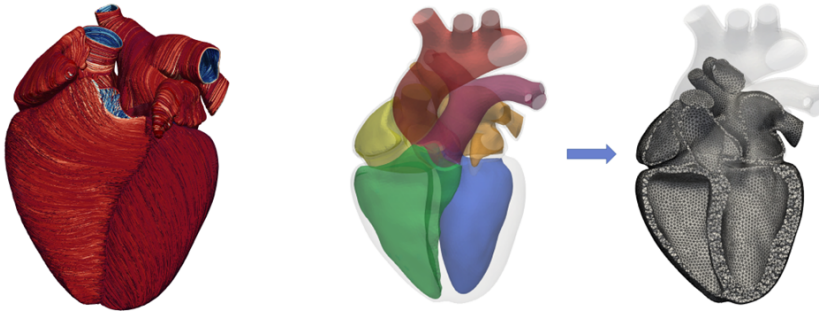


Fig. 5: Generation of cardiac fibers (left) and construction of the computational mesh (right) (credits: R. Piersanti and A. Zingaro Politecnico di Milano).

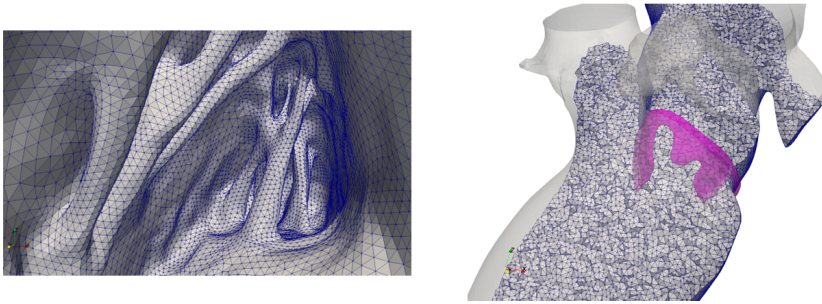


Fig. 6: Two examples of computational meshes for the cardiac modeling: Auricle cavity of the right atrium (left) and left heart (right) (credits: M. Fedele, Politecnico di Milano).

illustration, we will refer to spatial approximations based on the finite element method, whereas the time derivatives of the model will be discretized by suitable finite differences [54]. Purely as an example, Figure 5, right, illustrates how to obtain a three-dimensional mesh of the entire cardiac tissue; see [18]. As an example, Figure 6 shows a detail of the mesh in the auricle cavity of the right atrium (left) and of the left heart (right).

Needless to say, as N is unavoidably extremely large (often reaching hundreds of millions), supercomputers are necessary at this stage. Indeed, the simulation of a single heartbeat (about one second of physical time) may require several hours of computation on a big, modern supercomputer.

From a mathematician's perspective, mathematical and numerical models of the heart function represent an inexhaustible source of mathematical challenges. From an applied mathematician's perspective, the interest is further enhanced by the ambition to provide doctors with a "tool" that may help them with diagnosis and treatment. In the next section we will show in a few examples the way we can nowadays provide doctors with solutions of clinical relevance.

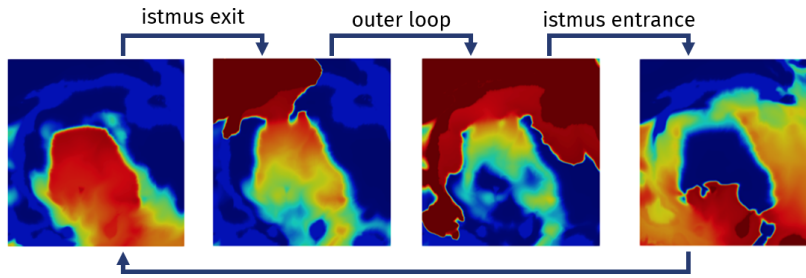


Fig. 7: Numerical simulation of a self-sustained reentry circuit (credits: S. Pagani, Politecnico di Milano) [21,23].

4 Some examples of clinical collaborations

In this section, we present some examples of applications of the cardiac function model presented above. Among the classes of diseases and possible associated therapies, we investigated those related to heart rhythm and conduction disorders, valve malfunction, and non-physiological cardiac perfusion, the treatment of which requires clinical procedures with high economic and social impact.

4.1 Quantitative understanding of arrhythmogenesis

Research activity, in collaboration with the cardiac arrhythmology and electrophysiology unit of IRCCS Ospedale San Raffaele in Milan and Humanitas Hospital in Milan, has provided quantitative insights into the factors that promote the initiation and maintenance of arrhythmias, such as post-ischemic ventricular tachycardia (VT) [22]. Structural abnormalities of the myocardium, generated by an episode of acute myocardial infarction, may set the stage for the formation of a reentry circuit near the scar area. Along such a circuit, the impulse can continue to reactivate the ventricles in an accelerated and uncontrolled manner, leading in some cases to cardiac arrest, a fatal condition if left untreated within a few minutes, which causes about 20 percent of deaths in Europe. The standard therapy for this type of condition consists of an electrophysiological study with transcatheter ablation. This procedure allows for the detection and elimination by radiofrequency delivery of those channels (isthmuses), which make up the re-entry circuit repeatedly traveled by the electrical pulse. Quantitative analysis of the data collected during this procedure allows the cardiologist to easily identify areas of high arrhythmic propensity, such as areas of slowing conduction or with abrupt change in the direction of pulse propagation (areas of high rotationality) [22]. Visualization of these indicators guides the cardiologist in identifying those areas in which to deliver radiofrequency (ablation targets). A similar procedure allows the treatment of atrial fibrillation (AF), a disorganization of pulse propagation in

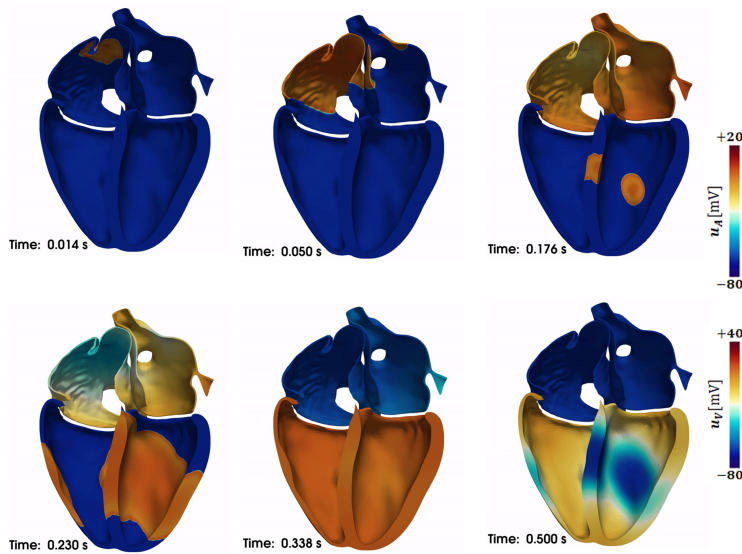


Fig. 8: Propagation of the action potential in a whole heart simulation (credits: R. Piersanti, Politecnico di Milano).

the atrium, which is the most common of arrhythmias and the most significant cardiac threat in Western countries in terms of morbidity and mortality. For this pathology too, the causes of induction and sustainment are to be found in progressive tissue damage, demonstrated quantitatively by the presence of more areas of slowing and high rotationality in patients with a persistent form, whose arrhythmic events are self-sustaining beyond 7 days [21, 23]. Numerical simulation of cardiac arrhythmias, however, is very difficult. The electrical potential presents a complex pattern with spiral waves or along reentrant circuits (Figure 7), unlike the orderly propagation typical of normal beating (Figure 8). Once originated, these mechanisms are self-sustaining and overpower the normal heart rhythm.

Mathematical models, through the integration of patients' electrical measurements, allow visualization and detailed analysis of reentry mechanisms and their evolution (which are difficult to measure in clinical practice). Simulation of localized reentry, based on data from patients with atrial fibrillation, has shown the role of heterogeneity in the conduction and refractoriness properties of the atrial myocardium in sustaining the arrhythmic event [49]. These indications along with new integrated approaches will be part of the continuous technological advancement aimed at improving ablation procedures.

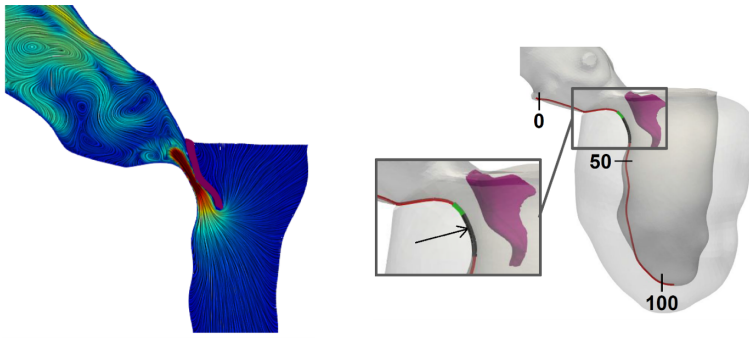


Fig. 9: Blood velocity in the left ventricle and aorta in presence of hypertrophic obstructive cardiomyopathy (left) and optimal region (in black) for myectomy (right) (credits: I. Fumagalli, Politecnico di Milano).

4.2 Guidance on interventricular septal myectomy

With the Luigi Sacco Hospital in Milan, we provide guidance on interventricular septal myectomy, the most widely used treatment for hypertrophic obstructive cardiomyopathy, which consists of thickening of the septum to such an extent that blood ejection from the left ventricle is difficult. The location of the best area to remove remains difficult to determine. With our study, we provide precise guidance to the cardiac surgeon on how to perform myectomy by noninvasive fluid dynamics analysis in the vicinity of the aortic valve. For example, in Figure 9 we show the velocity field over a section exiting the ventricle and the region identified as optimal to perform myectomy (in gray), being the one with the largest pressure gradients according to our study [24, 26].

4.3 Optimization of cardiac resynchronization therapy

In collaboration with the cardiology and radiology divisions of the S. Maria del Carmine Hospital in Rovereto, Italy, we have taken the first steps toward optimizing cardiac resynchronization therapy (CRT), which consists of implanting a device capable of restoring the correct synchrony of the heartbeat if it has been compromised by conduction disturbances or the presence of scarring. This is done by mapping the coronary veins of the left ventricle by inserting a catheter-electrode through the vessels of the circulation to detect electrical activity. The mapping is used to identify the point of latest activation where the left CRT electrode is placed. Our work has developed a mathematical tool that will be able to reduce mapping time and thus patient exposure time to invasive treatment, to calculate the point of latest activation [65, 70]. This allowed us to simulate CRT scenarios potentially exploring all epicardial veins and not just those mapped, see Figure 10.

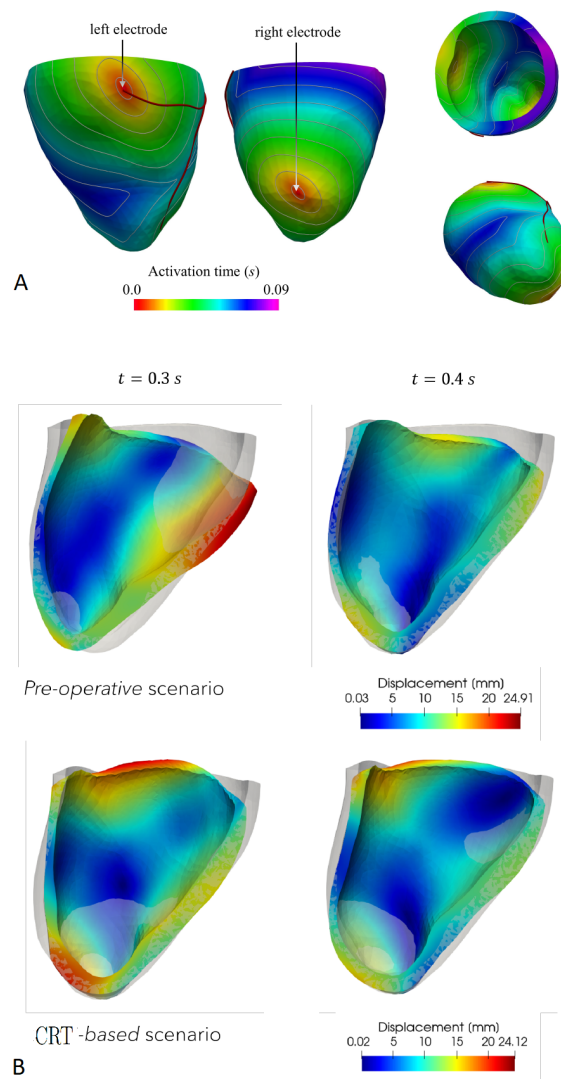


Fig. 10: A) Location of CRT electrodes; B) Comparison between cardiac contraction before (up) and after (bottom) CRT. Notice the restored synchrony of contraction in the CRT case (credits: S. Stella and E. Capuano).

4.4 Assessing cardiac perfusion under stress conditions

In collaboration with the Monzino Cardiology Center in Milan, Italy, we are instead collaborating on cardiac perfusion modeling. Here we study the fluid dynamics of large coronary arteries reconstructed from imaging coupled with a porous medium model to simulate smaller coronary arteries and microcircu-

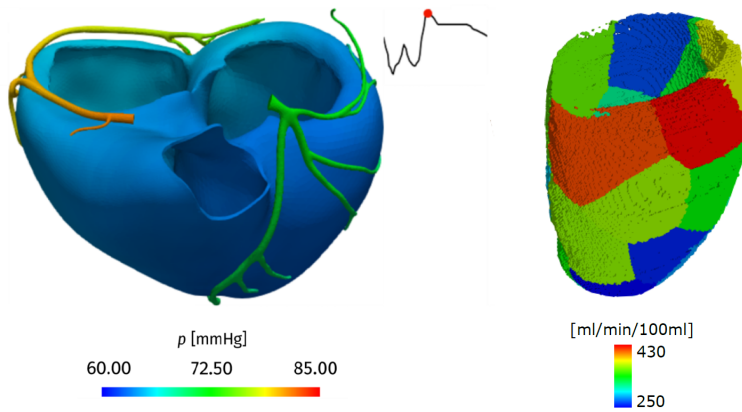


Fig. 11: Pressure field in the large coronaries and myocardial ventricles (left) and blood flow maps in the left ventricle (credits: S. Di Gregorio).

lation. This mathematical model makes it possible to calculate cardiac perfusion and thus assess what the effect of, for example, coronary artery stenosis is on blood supply in the various regions of the myocardium. The ambitious study we are conducting is to apply our model to patients whose perfusion has been assessed clinically by pharmacologically inducing a stress condition. Our method could then replace or otherwise support exercise testing by providing an alternative way to assess perfusion under stress conditions [15].

Figure 11 shows the pressure field in the coronaries and myocardium of a biventricular geometry (left) and perfusion in terms of myocardial blood flow maps in the left ventricle (right), obtained by numerical simulations of our perfusion model.

4.5 Optimization of transcatheter aortic valve implantation

With the Monzino Cardiology Center in Milan, we study the operation of a catheter-implanted prosthetic aortic valve (TAVI), an increasingly popular treatment against aortic stenosis. Years after TAVI implantation, the prosthetic valve leaflets may undergo structural valvular deterioration, due to calcification or weakening of tissue, augmenting the risk of aortic re-stenosis, which may require a new operation. By integrating clinical data and mathematical models of the interaction between blood flow and prosthesis structure, we can identify predictive indicators of risk even before surgery, to aid physician decisions about surgery and post-implantation monitoring of the patient [25].

Figure 12 shows the time-average systolic wall shear stress exerted by blood flow on the walls of the aorta of 5 patients: we observed that this indicator allows us to discriminate between patients who will undergo SVD and others who will not experience prosthesis degeneration.

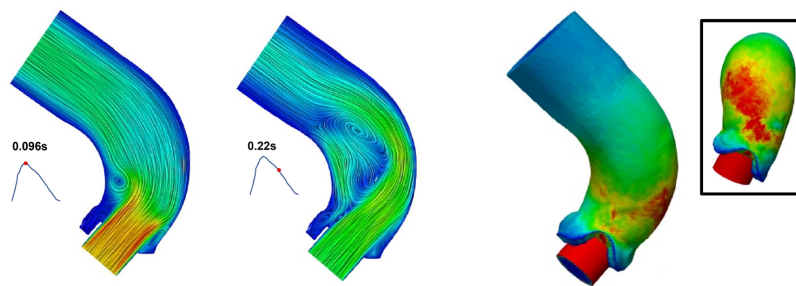


Fig. 12: Velocity field in the aorta at two time instants (left) and peak Wall Shear Stress (right). TAVI simulation (credits: R. Polidori and F. Renzi).

5 Conclusions

Computational Medicine is still in its infancy. It would be ungenerous to have very high expectations in a very short time. However, in this paper we have tried to explain what its foundational elements are and, through a few examples, show that even now we can find results that enable us to attract the interest of physicians. We believe that the potential for improvement is very high and that it represents a great opportunity to combine medical knowledge with the power that mathematics and computational science offer us. The last three decades have witnessed the explosion of clinical imaging. Refined tools such as tomography, MRI, cine MRI and DT-MRI, certainly considered strangers in the beginning, are now valuable companions. Our belief is that mathematical models will be their natural continuation: they match perfectly with the former and will become essential complements of investigation in the diagnostic and therapeutic phases. They do not require high investment costs, are noninvasive and allow them to be used in the predictive phase as well.

Before concluding, we would like to note that an important mission of our studies is that of inter-disciplinary education. In fact, we intend to intercept the growing demand for training of a new professional profile at the interface between medicine, bioengineering and mathematics, an expert in Computational Medicine who can give support to medical decision-making, thanks to the conscious use of advanced mathematical tools.

Acknowledgements We would like to thank Professor Antonio Corno of the Children's Heart Institute, Children's Memorial Hermann Hospital and McGovern Medical School in Houston, Professor Paolo Della Bella of I.R.C.C.S. San Raffaele Hospital in Milan and Dr. Antonio Frontera of Humanitas Research Hospital, Dr. Roberto Scrofani of the Policlinico Ca' Granda Hospital in Milan, Drs. Gianluca Pontone and Laura Fusini of the Monzino Cardiology Center in Milan, Drs. Maurizio Del Greco and Domenico Catanzariti of the S. Maria del Carmine Hospital in Rovereto.

Conflict of interest

The authors declare that they have no conflict of interest.

References

1. Abraham, W.T., Hayes, D.L.: Cardiac resynchronization therapy for heart failure. *Circulation* **108**(21), 2596–2603 (2003)
2. Arevalo, H.J., Vadakkumpadan, F., Guallar, E., Jebb, A., Malamas, P., Wu, K.C., Trayanova, N.A.: Arrhythmia risk stratification of patients after myocardial infarction using personalized heart models. *Nature communications* **7**(1), 1–8 (2016)
3. Augustin, C.M., Neic, A., Liebmann, M., Prassl, A.J., Niederer, S.A., Haase, G., Plank, G.: Anatomically accurate high resolution modeling of human whole heart electromechanics: A strongly scalable algebraic multigrid solver method for nonlinear deformation. *Journal of Computational Physics* **305**, 622–646 (2016). DOI 10.1016/j.jcp.2015.10.045
4. Basting, S., Quaini, A., Čanić, S., Glowinski, R.: Extended ale method for fluid–structure interaction problems with large structural displacements. *Journal of Computational Physics* **331**, 312–336 (2017)
5. Bayer, J., Blake, R., Plank, G., Trayanova, N.: A novel rule-based algorithm for assigning myocardial fiber orientation to computational heart models. *Annals of Biomedical Engineering* **40**(10), 2243–2254 (2012)
6. Bazilevs, Y., Calo, V., Cottrell, J., Hughes, T., Reali, A., Scovazzi, G.: Variational multiscale residual-based turbulence modeling for large eddy simulation of incompressible flows. *Computer methods in applied mechanics and engineering* **197**(1–4), 173–201 (2007)
7. Blanco, P.J., Feijóo, R.A.: A 3D–1D–0D Computational Model for the Entire Cardiovascular System. *Computational Mechanics* **24**, 5887–5911 (2010)
8. Bucelli, M., Zingaro, A., Africa, P.C., Fumagalli, I., Dede, L., Quarteroni, A.: A mathematical model that integrates cardiac electrophysiology, mechanics and fluid dynamics: application to the human left heart. *arXiv preprint arXiv:2208.05551* (2022)
9. Chabiniok, R., Wang, V., Hadjicharalambous, M., Asner, L., Lee, J., Sermesant, M., Kuhl, E., Young, A., Moireau, P., Nash, M., Chapelle, D., Nordsletten, D.: Multiphysics and multiscale modelling, data–model fusion and integration of organ physiology in the clinic: ventricular cardiac mechanics. *Interface Focus* **6**(2), 20150083 (2016)
10. Colli Franzone, P., Pavarino, L.F., Scacchi, S.: *Mathematical Cardiac Electrophysiology*. Springer (2014)
11. Cookson, A., Lee, J., Michler, C., Chabiniok, R., Hyde, E., Nordsletten, D., Sinclair, M., Siebes, M., Smith, N.: A novel porous mechanical framework for modelling the interaction between coronary perfusion and myocardial mechanics. *Journal of biomechanics* **45**(5), 850–855 (2012)
12. Crampin, E.J., Halstead, M., Hunter, P., Nielsen, P., Noble, D., Smith, N., Tawhai, M.: Computational physiology and the physiome project. *Experimental Physiology* **89**(1), 1–26 (2004)
13. Del Corso, G., Verzicco, R., Viola, F.: A fast computational model for the electrophysiology of the whole human heart. *Journal of Computational Physics* **457**, 111084 (2022). DOI <https://doi.org/10.1016/j.jcp.2022.111084>
14. Di Gregorio, S., Fedele, M., Pontone, G., Corno, A.F., Zunino, P., Vergara, C., Quarteroni, A.: A computational model applied to myocardial perfusion in the human heart: from large coronaries to microvasculature. *Journal of Computational Physics* **424**, 109836 (2021)
15. Di Gregorio, S., Vergara, C., Pelagi, G.M., Baggiano, A., Zunino, P., Guglielmo, M., Fusini, L., Muscogiuri, G., Rossi, A., Rabbat, M.G., et al.: Prediction of myocardial blood flow under stress conditions by means of a computational model. *European Journal of Nuclear Medicine and Molecular Imaging* **49**(6), 1894–1905 (2022)
16. Fedele, M., Faggiano, E., Dedè, L., Quarteroni, A.: A patient-specific aortic valve model based on moving resistive immersed implicit surfaces. *Biomechanics and modeling in mechanobiology* **16**(5), 1779–1803 (2017)

17. Fedele, M., Piersanti, R., Regazzoni, F., Salvador, M., Africa, P.C., Bucelli, M., Zingaro, A., Dede, L., Quarteroni, A.: A comprehensive and biophysically detailed computational model of the whole human heart electromechanics. arXiv preprint arXiv:2207.12460 (2022)
18. Fedele, M., Quarteroni, A.: Polygonal surface processing and mesh generation tools for the numerical simulation of the cardiac function. *International Journal for Numerical Methods in Biomedical Engineering* **37**(4), e3435 (2021). DOI 10.1002/cnm.3435
19. Fink, M., Niederer, S., Cherry, E., Fenton, F., Koivumäki, J., Seemann, G., Thul, R., Zhang, H., Sachse, F., Beard, D., Crampin, E., Smith, N.: Cardiac cell modelling: observations from the heart of the cardiac physiome project. *Progress in Biophysics and Molecular Biology* **104**(1), 2–21 (2011)
20. Forti, D., Dedè, L.: Semi-implicit bdf time discretization of the navier–stokes equations with vms-les modeling in a high performance computing framework. *Computers & Fluids* **117**, 168–182 (2015)
21. Frontera, A., Limite, L., Pagani, S., Cireddu, M., Vlachos, K., et al.: Electrogram fractionation during sinus rhythm occurs in normal voltage atrial tissue in patients with atrial fibrillation. *Pacing and Clinical Electrophysiology* **45**(2), 219–228 (2022)
22. Frontera, A., Pagani, S., Limite, L., Hadjis, A., Manzoni, A., Dede, L., Quarteroni, A., Della Bella, P.: Outer loop and isthmus in ventricular tachycardia circuits: Characteristics and implications. *Heart Rhythm* **17**(10), 1719–1728 (2020)
23. Frontera, A., Pagani, S., Limite, L.R., Peirone, A., Fioravanti, F., Enache, B., Cuelar Silva, J., Vlachos, K., Meyer, C., Montesano, G., et al.: Slow conduction corridors and pivot sites characterize the electrical remodeling in atrial fibrillation. *JACC Clinical Electrophysiology* **8**(5), 561–577 (2022). DOI 10.1016/j.jacep.2022.01.019
24. Fumagalli, I., Fedele, M., Vergara, C., Ippolito, S., Nicolò, F., Antona, C., Scrofani, R., Quarteroni, A., et al.: An image-based computational hemodynamics study of the systolic anterior motion of the mitral valve. *Computers in Biology and Medicine* **123**, 103922 (2020)
25. Fumagalli, I., Polidori, R., Renzi, F., Fusini, L., Quarteroni, A., Pontone, G., Vergara, C.: Fluid-structure interaction analysis of transcatheter aortic valve implantation. MOX Report n.29 (2022)
26. Fumagalli, I., Vitullo, P., Vergara, C., Fedele, M., Corno, A.F., Ippolito, S., Scrofani, R., Quarteroni, A.: Image-based computational hemodynamics analysis of systolic obstruction in hypertrophic cardiomyopathy. *Frontiers in Physiology* p. 2437 (2022)
27. Genet, M., Lee, L.C., Baillargeon, B., Guccione, J.M., Kuhl, E.: Modeling pathologies of diastolic and systolic heart failure. *Annals of biomedical engineering* **44**(1), 112–127 (2016)
28. Gerach, T., Schuler, S., Fröhlich, J., Lindner, L., Kovacheva, E., Moss, R., Wülfers, E.M., Seemann, G., Wieners, C., Loewe, A.: Electro-Mechanical Whole-Heart Digital Twins: A Fully Coupled Multi-Physics Approach. *Mathematics* **9**(11), 1247 (2021). DOI 10.3390/math9111247
29. Glass, L., Hunter, P., McCulloch, A.: *Theory of heart: biomechanics, biophysics, and nonlinear dynamics of cardiac function*. Springer Science & Business Media (2012)
30. Göktepe, S., Kuhl, E.: Electromechanics of the heart: a unified approach to the strongly coupled excitation-contraction problem. *Computational Mechanics* **45**, 227–243 (2010)
31. Gray, R.A., Pathmanathan, P.: Patient-specific cardiovascular computational modeling: diversity of personalization and challenges. *Journal of cardiovascular translational research* **11**(2), 80–88 (2018)
32. Griffith, B.E., Peskin, C.S.: *Electrophysiology*. *Communications on Pure and Applied Mathematics* **66**(12), 1837–1913 (2013). DOI <https://doi.org/10.1002/cpa.21484>
33. Guccione, J.M., McCulloch, A.D.: Finite element modeling of ventricular mechanics. In: *Theory of Heart*, pp. 121–144. Springer (1991)
34. Guccione, J.M., McCulloch, A.D., Waldman, L.K.: Passive material properties of intact ventricular myocardium determined from a cylindrical model. *Journal of Biomechanical Engineering* **113**, 42–55 (1991)
35. Hirschvogel, M., Bassilious, M., Jagschies, L., et al.: A monolithic 3D–0D coupled closed-loop model of the heart and the vascular system: Experiment-based parameter estimation for patient-specific cardiac mechanics. *International Journal for Numerical Methods in Biomedical Engineering* **33**(8), e2842 (2017)

36. Holzapfel, G.A., Ogden, R.W.: Constitutive modelling of passive myocardium: a structurally based framework for material characterization. *Mathematical, Physical and Engineering Sciences* **367**, 3445–3475 (2009)
37. Huyghe, J.M., Van Campen, D.H.: Finite deformation theory of hierarchically arranged porous solids—i. balance of mass and momentum. *International journal of engineering science* **33**(13), 1861–1871 (1995)
38. Jianhai, Z., Dapeng, C., Shengquan, Z.: Ale finite element analysis of the opening and closing process of the artificial mechanical valve. *Applied Mathematics and Mechanics* **17**(5), 403–412 (1996)
39. Jung, A., Gsell, M., Augustin, C., Plank, G.: An integrated workflow for building digital twins of cardiac electromechanics—a multi-fidelity approach for personalising active mechanics. *Mathematics* **10**(5) (2022)
40. Karabelas, E., Longobardi, S., Fuchsberger, J., Razeghi, O., Rodero, C., Strocchi, M., Rajani, R., Haase, G., Plank, G., Niederer, S.: Global sensitivity analysis of four chamber heart hemodynamics using surrogate models. *IEEE Transactions on Biomedical Engineering* pp. 1–1 (2022)
41. Katz, A.M.: *Physiology of the Heart*. Lippincott Williams & Wilkins (2010)
42. Klabunde, R.: *Cardiovascular physiology concepts*. Lippincott Williams & Wilkins (2011)
43. Land, S., Niederer, S.A.: Influence of atrial contraction dynamics on cardiac function. *International Journal for Numerical Methods in Biomedical Engineering* **34**(3), e2931 (2018). DOI 10.1002/cnm.2931
44. Mitchell, J.R., Wang, J.J.: Expanding application of the Wiggers diagram to teach cardiovascular physiology. *Advances in physiology education* **38**(2), 170–175 (2014)
45. Mittal, R., Seo, J.H., Vedula, V., Choi, Y.J., Liu, H., Huang, H.H., Jain, S., Younes, L., Abraham, T., George, R.T.: Computational modeling of cardiac hemodynamics: Current status and future outlook. *J. Comput. Phys.* **305**, 1065–1082 (2016). DOI 10.1016/j.jcp.2015.11.022
46. Niederer, S.A., Lumens, J., Trayanova, N.A.: Computational models in cardiology. *Nature Reviews Cardiology* **16**(2), 100–111 (2019). DOI 10.1038/s41569-018-0104-y
47. Nordsletten, D., Niederer, S., Nash, M., Hunter, P., Smith, N.: Coupling multi-physics models to cardiac mechanics. *Progress in Biophysics and Molecular Biology* **104**(1-3), 77–88 (2011)
48. Ogden, R.: *Non-linear elastic deformations*. Dover Publications (1997)
49. Pagani, S., Dede', L., Frontera, A., Salvador, M., Limite, L., et al.: A computational study of the electrophysiological substrate in patients suffering from atrial fibrillation. *Frontiers in Physiology* **12**, 673612 (2021)
50. Peirlinck, M., Yao, J., Sahli Costabal, F., Kuhl, E.: How drugs modulate the performance of the human heart. *Comput. Mech.* (2022). DOI 10.1007/s10237-021-01421-z
51. Peskin, C.S.: Flow patterns around heart valves: A numerical method. *Journal of Computational Physics* **10**(2), 252–271 (1972)
52. Pfaller, M.R., Hörmann, J.M., Weigl, M., Nagler, A., Chabiniok, R., Bertoglio, C., Wall, W.A.: The importance of the pericardium for cardiac biomechanics: from physiology to computational modeling. *Biomechanics and Modeling in Mechanobiology* **18**(2), 503–529 (2019). DOI 10.1007/s10237-018-1098-4
53. Piersanti, R., Africa, P.C., Fedele, M., Vergara, C., Dedè, L., Corno, A.F., Quarteroni, A.: Modeling cardiac muscle fibers in ventricular and atrial electrophysiology simulations. *Computer Methods in Applied Mechanics and Engineering* **373**, 113468 (2021)
54. Quarteroni, A.: *Numerical models for differential problems*. Springer (2017)
55. Quarteroni, A., Dede', L., Manzoni, A., Vergara, C.: *Mathematical Modelling of the Human Cardiovascular System: Data, Numerical Approximation, Clinical Applications*. Cambridge University Press (2019)
56. Quarteroni, A., Lassila, T., Rossi, S., Ruiz-Baier, R.: Integrated heart - coupling multiscale and multiphysics models for the simulation of the cardiac function. *Computer Methods in Applied Mechanics and Engineering* **314**, 345–407 (2017)
57. Regazzoni, F., Dedè, L., Quarteroni, A.: Biophysically detailed mathematical models of multiscale cardiac active mechanics. *PLOS Computational Biology* **16**(10), e1008294 (2020). DOI 10.1371/journal.pcbi.1008294

58. Regazzoni, F., Dedè, L., Quarteroni, A.: Active force generation in cardiac muscle cells: mathematical modeling and numerical simulation of the actin-myosin interaction. *Vietnam Journal of Mathematics* **49**, 87–118 (2021)
59. Regazzoni, F., Salvador, M., Africa, P., Fedele, M., Dedè, L., Quarteroni, A.: A cardiac electromechanical model coupled with a lumped-parameter model for closed-loop blood circulation. *Journal of Computational Physics* **457**, 111083 (2022). DOI 10.1016/j.jcp.2022.111083
60. Regazzoni, F., Salvador, M., Dedè, L., Quarteroni, A.: A machine learning method for real-time numerical simulations of cardiac electromechanics. *Computer Methods in Applied Mechanics and Engineering* **393**, 114825 (2022)
61. Salvador, M., Regazzoni, F., Pagani, S., Dedè, L., Trayanova, N., Quarteroni, A.: The role of mechano-electric feedbacks and hemodynamic coupling in scar-related ventricular tachycardia. *Computers in Biology and Medicine* p. 105203 (2022)
62. Santiago, A., Aguado-Sierra, J., Zavala-Aké, M., Doste-Beltran, R., Gómez, S., Arís, R., Cajas, J.C., Casoni, E., Vázquez, M.: Fully coupled fluid-electro-mechanical model of the human heart for supercomputers. *International Journal for Numerical Methods in Biomedical Engineering* **34**(12), e3140 (2018). DOI 10.1002/cnm.3140
63. Smith, N., Nickerson, D., Crampin, E., Hunter, P.: Multiscale computational modelling of the heart. *Acta Numerica* **13**, 371–431 (2004)
64. Smith, N.P., Nickerson, D.P., Crampin, E.J., et al.: Multiscale computational modelling of the heart. *Acta Numerica* **13**, 371–431 (2004)
65. Stella, S., Vergara, C., Maines, M., Catanzariti, D., Africa, P.C., Demattè, C., Centonze, M., Nobile, F., Del Greco, M., Quarteroni, A.: Integration of activation maps of epicardial veins in computational cardiac electrophysiology. *Computers in Biology and Medicine* **127**, 104047 (2020)
66. Sugiura, S., Okada, J., Washio, T., Hisada, T.: *UT-Heart: A Finite Element Model Designed for the Multiscale and Multiphysics Integration of our Knowledge on the Human Heart*, pp. 221–245. Springer US, New York, NY (2022)
67. Tomek, J., Bueno-Orovio, A., Passini, E., Zhou, X., Mincholé, A., Britton, O., Bartolucci, C., Severi, S., Shrier, A., Virag, L., Varro, A., Rodriguez, B.: Development, calibration, and validation of a novel human ventricular myocyte model in health, disease, and drug block. *eLife* **8**, e48890 (2019)
68. Trayanova, N., Rice, J.: Cardiac electromechanical models: from cell to organ. *Frontiers in Physiology* **2**, 43 (2011)
69. Trayanova, N.A.: Computational cardiology: the heart of the matter. *International Scholarly Research Notices* **2012** (2012). DOI 10.5402/2012/269680
70. Vergara, C., Stella, S., Maines, M., Africa, P.C., Catanzariti, D., Demattè, C., Centonze, M., Nobile, F., Quarteroni, A., Del Greco, M.: Computational electrophysiology of the coronary sinus branches based on electro-anatomical mapping for the prediction of the latest activated region. *Medical & Biological Engineering & Computing* **60**(8), 2307–2319 (2022)
71. Verzicco, R.: Electro-fluid-mechanics of the heart. *Journal of Fluid Mechanics* **941** (2022)
72. Viola, F., Meschini, V., Verzicco, R.: Fluid–structure–electrophysiology interaction (fsei) in the left-heart: a multi-way coupled computational model. *European Journal of Mechanics-B/Fluids* **79**, 212–232 (2020). DOI 10.1016/j.euromechflu.2019.09.006
73. Washio, T., Okada, J.i., Takahashi, A., Yoneda, K., Kadooka, Y., Sugiura, S., Hisada, T.: Multiscale heart simulation with cooperative stochastic cross-bridge dynamics and cellular structures. *Multiscale Modeling & Simulation* **11**(4), 965–999 (2013)
74. Zingaro, A., Fumagalli, I., Dedè, L., Fedele, M., Africa, P.C., Corno, A.F., Quarteroni, A.: A geometric multiscale model for the numerical simulation of blood flow in the human left heart. *Discrete and Continuous Dynamical Systems-S* **15**(8), 2391–2427 (2022)
75. Zingaro, A., Menghini, F., Quarteroni, A., et al.: Hemodynamics of the heart’s left atrium based on a variational multiscale-les numerical method. *European Journal of Mechanics-B/Fluids* **89**, 380–400 (2021)

MOX Technical Reports, last issues

Dipartimento di Matematica
Politecnico di Milano, Via Bonardi 9 - 20133 Milano (Italy)

- 02/2023** Boon, W. M.; Fumagalli, A.; Scotti, A.
Mixed and multipoint finite element methods for rotation-based poroelasticity
- 03/2023** Africa, P.C.; Perotto, S.; de Falco, C.
Scalable Recovery-based Adaptation on Quadtree Meshes for Advection-Diffusion-Reaction Problems
- 01/2023** Zingaro, A.; Bucelli, M.; Piersanti, R.; Regazzoni, F.; Dede', L.; Quarteroni, A.
An electromechanics-driven fluid dynamics model for the simulation of the whole human heart
- 82/2022** Ciaramella, G.; Gander, M.; Van Criekingen, S.; Vanzan, T.
A PETSc Parallel Implementation of Substructured One- and Two-level Schwarz Methods
- 81/2022** Bonizzoni, F.; Hauck, M.; Peterseim, D.
A reduced basis super-localized orthogonal decomposition for reaction-convection-diffusion problems
- 84/2022** Ciaramella, G.; Gambarini, M.; Miglio, E.
A preconditioner for free-surface hydrodynamics BEM
- 85/2022** Lurani Cernuschi, A.; Masci, C.; Corso, F.; Muccini, C.; Ceccarelli, D.; San Raffaele Hospital
Galli, L.; Ieva, F.; Paganoni, A.M.; Castagna, A.
A neural network approach to survival analysis for modelling time to cardiovascular diseases in HIV patients with longitudinal observations
- 83/2022** Ciaramella, G.; Gander, M.; Mazzieri, I.
Unmapped tent pitching schemes by waveform relaxation
- 80/2022** Balduzzi, G.; Bonizzoni, F.; Tamellini, L.
Uncertainty quantification in timber-like beams using sparse grids: theory and examples with off-the-shelf software utilization
- 78/2022** Bucelli, M.; Gabriel, M. G.; Gigante, G.; Quarteroni, A.; Vergara, C.
A stable loosely-coupled scheme for cardiac electro-fluid-structure interaction